Progress In Electromagnetics Research C, Vol. 8, 149–160, 2009

MICROWAVE ABSORPTION, CONDUCTIVITY AND COMPLEX PEMITTIVITY OF FRITLESS $Ni_{(1-x)}Cu_xMn_2O_4$ $(0 \leq x \leq 1)$ CERAMIC THICK FILM: EFFECT OF COPPER

R. N. Jadhav and V. Puri

Thick and Thin Film Device Lab, Department of Physics
Shivaji University
Kolhapur 416004, India

Abstract—The effect of copper on the microwave absorption, conductivity and complex permittivity of fritless $Ni_{(1-x)}Cu_xMn_2O_4$ $(x = 0, 0.4, 0.8, 1)$ thick film on alumina have been investigated in the 8–18 GHz frequency range. The structural changes have been identified by scanning electron microscope (SEM), FTIR and RAMAN scattering spectroscopy. The microwave conductivity and permittivity increase as copper content increases. The fritless $Ni_{(1-x)}Cu_xMn_2O_4$ $(0 \leq x \leq 1)$ thick film with $x = 0.4$ shows best absorption properties, though all the other compositions also show good absorption in a large frequency range. The microwave conductivity increases from 1 S/cm to 951 S/cm due to copper and the dielectric constant $(\acute{\varepsilon})$ increases from 7 to 19.5.

1. INTRODUCTION

Due to the proliferation in the use of the electromagnetic wave especially the radio frequency for a variety of applications the problem of electromagnetic wave pollution has attracted the attention of researchers. Materials which can absorb microwaves can eliminate electromagnetic wave pollution. Wide spread applications of electromagnetic absorbers have inspired engineers to explore optimal design with available algorithms. Ideally a thin, light weight and wideband absorber is an optimum one [1]. The main mechanism of microwave absorber is purely dielectric, polarization and conductive losses [2]. Dielectric material for microwave applications should in general satisfy three requirements: high dielectric constant,

Corresponding author: V. Puri (vrp_phy@unishivaji.ac.in).

low dielectric loss and small temperature coefficient of resonant frequency [3]. Many techniques have been developed to measure the permittivity [4, 5]. The complex permittivity is an important factor which can be altered to achieve maximum absorption of the electromagnetic waves. Permittivity relates to the material's ability to transmit (or permit) an electric field. Permittivity also depends on the physical properties such as density and composition of the material, and it changes with temperature and frequency.

Thick film technology has been proved to be cost effective method highly conducive to planarization. Thick film thermistor is a device that can be used in high frequency range. This is possible due to the development of new thick film thermistor material [6]. Nickel manganite has an intermediate cubic structure consisting 3d transition metals which have negative temperature coefficient (NTC) [7]. The composition of solid solution of 3d strongly affects the distribution of cations and thus change the properties [8, 9]. Oxalate co-precipitation method [10] can be used to synthesize single phase, homogeneous, fine grained ceramic.

In this paper, we report the effect of copper content on the microwave properties of fritless (glass free) $Ni_{(1-x)}Cu_xMn_2O_4$ ($0 \leq x \leq 1$) thick film NTC ceramic. $Ni_{(1-x)}Cu_xMn_2O_4$ ($0 \leq x \leq 1$) was prepared by oxalic precursor method. Effect of copper content in the nickel manganite thick film was also studied by structural characterization using X-ray diffraction spectroscopy (XRD), Fourier transform infrared (FTIR), RAMAN spectroscopy and Scanning electron microscope (SEM).

2. EXPERIMENTAL PROCEDURE

The $Ni_{(1-x)}Cu_xMn_2O_4$ ($0 \leq x \leq 1$) powder was prepared by oxalic precursor method using nickel acetate, manganese acetate, copper acetate of definite proportion mixed with 2 M hot oxalic acid solution with constant stirring. The chemicals were weighted according to required stoichiometry proportion by varying $x = 0$, 0.4, 0.8, 1. The prepared precipitate was filtered, washed with distilled water and dried at 400°C and finally sintered at 1000°C for 8 Hrs.

Thick film paste was prepared by mixing in agate mortar 80 wt% of the ceramic powder, 12 wt% of inorganic binder (75 wt% Bi_2O_3 and 25% PbO) and organic vehicle (8 wt%) for 2 Hrs. The organic vehicle was a solution of ethyl cellulose and [2-(2-butoxyethoxy) ethyl]-acetate. The fritless $Ni_{(1-x)}Cu_xMn_2O_4$ ($0 \leq x \leq 1$) thick film was delineated on 96% alumina by screen printing and firing at 900°C in zonal furnace for 1 Hr. The thickness of the $Ni_{(1-x)}Cu_xMn_2O_4$ ($x = 0.0, 0.4, 0.8, 1$)

thick films which has rectangular shape with 1.1 cm width and 2.5 cm in height is $\sim 14\,\mu$m was obtained from gravimetric method.

The formation of spinel structure was confirmed by XRD using Cu-Kα radiation, ($\lambda = 1.541838$ A^0) (Philips Diffractometer PW 3710), structural changes observed by FTIR (Perkin-Elmer200), RAMAN (Bruker, Multi-RAMAN spectrometer (RAM-II)), surface morphological studied by SEM (JSM-6360 JEOL, Japan).

Transmission of microwaves due to thick film was measured point by point using transmission/reflection method with rectangular waveguide, consisting of the X and Ku band generator, isolator, attenuator, directional coupler and RF detector. The composition dependent permittivity was measured in microwave frequency region 8.2 GHz to 18 GHz (X and Ku band) by VSWR method.

3. RESULTS AND DISCUSSIONS

The typical XRD pattern of $Ni_{(1-x)}Cu_xMn_2O_4$ ($x = 0,\ 0.4,\ 1$) thick film is shown in Fig. 1. It is observed that polycrystalline $Ni_{(1-x)}Cu_xMn_2O_4$ ($0 \leq x \leq 1$) was formed with dominant (311) plane which confirmed spinel structure. All peaks appearing in XRD pattern for $Ni_{(1-x)}Cu_xMn_2O_4$ ($0 \leq x \leq 1$) are very sharp indicating that the samples have high crystallinity. The miller index for each peak was determined based on a spinel structure of space group Fd3m.

Figure 2 shows the SEM (JSM-6360 JEOL Japan) morphology of thick film $Ni_{(1-x)}Cu_xMn_2O_4$ ($0 \leq x \leq 1$). It is seen that as copper content increases grain size also increases from $\sim 0.55\,\mu$m (for $x = 0.4$) to $\sim 1.3\,\mu$m (for $x = 0.8$). This might be due to higher atomic mobility

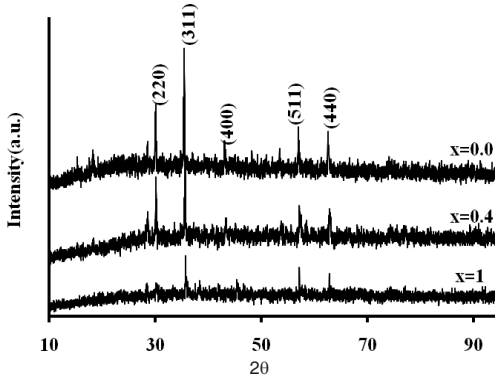

Figure 1. X-ray diffraction pattern of fritless $Ni_{(1-x)}Cu_xMn_2O_4$ thick film.

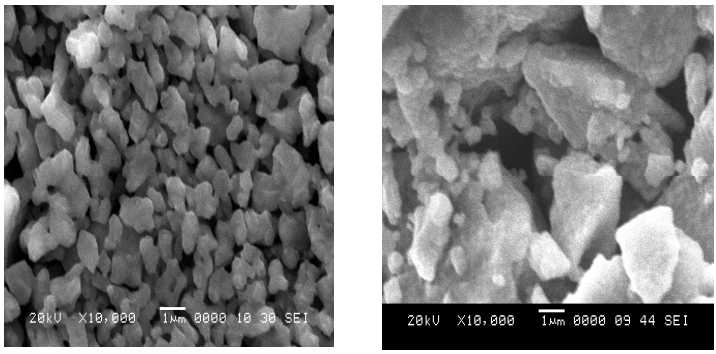

(a) (b)

Figure 2. SEM images of fritless $Ni_{(1-x)}Cu_xMn_2O_4$ thick films of (a) $x = 0.4$ and (b) $x = 0.8$.

of Cu ions induced by liquid phase sintering. It is observed that these thick films have larger porosity and open (thinner) grain boundaries with agglomeration. The voids appear to be more pronounced in the films with higher copper content. This may be due to the fact that copper being a metal; it prevents the formation of dense microstructure of fired thick film.

To further explore the doping effect of copper in the fritless $NiMn_2O_4$ thick film, vibration modes have been studied by means of FTIR and RAMAN spectra measurements because vibration modes are sensitive to substitution. In FTIR spectra (Fig. 3) two strong peaks were observed around $600\,cm^{-1}$ and $500\,cm^{-1}$. This confirmed the formation of spinel structure. As copper content increases the peak at $605\,cm^{-1}$ shifts to $600\,cm^{-1}$. This might be because the valance of Cu is smaller than Ni due to which the force constant of CuO_6 are smaller than NiO_6 octahedron [11]. The peak around $510\,cm^{-1}$ shifts to $496\,cm^{-1}$ due to the increase in copper content indicating decrease in frequency since the heavier Cu ions are substituted for Ni.

Figure 4 shows the RAMAN spectra (RS) of fritless $Ni_{(1-x)}Cu_xMn_2O_4$ ($x = 0, 0.4, 1$) thick film. It is observed that polycrystalline $NiMn_2O_4$ ($x = 0$) thick film is dominated by a strong broad band with peak centered at $645\,cm^{-1}$ and $515\,cm^{-1}$. A band with medium intensity appears at $559\,cm^{-1}$, while three bands are observed in low frequency region $388\,cm^{-1}$, $297\,cm^{-1}$ and $170\,cm^{-1}$, having weak intensity. In spinel oxides and other manganese oxides energies of $\sim$ 600–650 cm^{-1} are characteristics of vibrations involving the motion of oxygen atoms inside the octahedral unit MnO_6 [12].

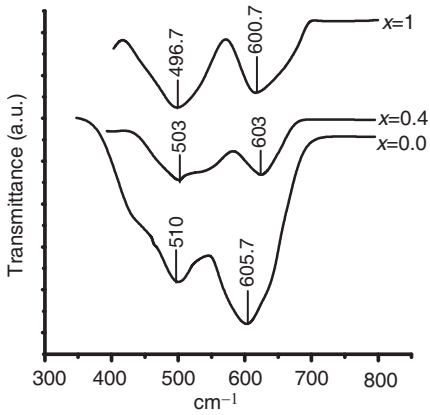

Figure 3. FTIR spectra of fritless $Ni_{(1-x)}Cu_xMn_2O_4$ thick film.

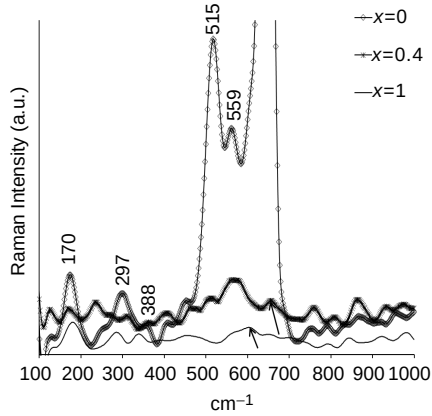

Figure 4. RAMAN spectra of fritless $Ni_{(1-x)}Cu_xMn_2O_4$ thick film.

Analysis of the vibrational spectra of $NiMn_2O_4$ and $CuMn_2O_4$ with Fd3m space group yields five modes which are RAMAN active $A_{1g}+E_g+3F_{2g}$. The RAMAN band located at about 645 cm^{-1} is viewed as a symmetric Mn-O stretching vibration of MnO_6 group. This high wave number band is assigned to the A_{1g} species in the O_h^7 spectroscopic symmetry. The RS peak at 297 cm^{-1} derives from the E_g symmetry whereas the peaks located at 170 cm^{-1}, 388 cm^{-1}, 559 cm^{-1} derives from F_{2g} species. Similar spectra have been observed in $LiMn_2O_4$ [13]. Dokko et al. [14] have reported that the peak intensity at $\sim$515 cm^{-1} is sharper due to nickel content and it is attributed to Ni^{2+}-O stretching mode in structure. As copper content increases RAMAN spectra shifts towards lower frequency (peaks shown by arrow). At $x = 0$ it is 645 cm^{-1}, at $x = 0.4$ it is 636 cm^{-1} and for $x = 1$ it is 600 cm^{-1} which is due to the heavier Cu ions substituted for Ni ions. The reduction of the intensity of this mode is due to the decrease of Jahn-Teller distortions in the averaged structure introduced by the smaller Cu ions [15] (ionic radii of $Cu^{2+} = 0.70$ Å and $Ni^{2+} = 0.78$ Å) [16].

The transmission and reflection of fritless $Ni_{(1-x)}Cu_xMn_2O_4$ ($0 \leq x \leq 1$) thick films was measured by the rectangular waveguide reflectometer set up shown in Fig. 5. The microwaves incident on the device under test were in the frequency range 8 GHz to 18 GHz. The waveguide reflectometer set up consists of Gunn oscillator, isolator, attenuator, two 3 dB directional couplers connected in reverse

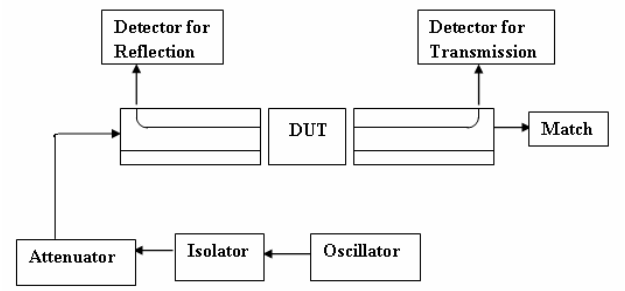

Figure 5. Schematic of microwave experimental setup for transmission and reflection of fritless $Ni_{(1-x)}Cu_xMn_2O_4$ thick film.

directions, sample holder for DUT (Device Under Test) and the diode detector. The system was calibrated by measuring the output with and without the DUT. The transmission and reflection of standard alumina sample was measured and found to be $\sim 70\%$ transmittance and $\sim 12\%$ reflectance in the 8–18 GHz frequency range.

The microwave insertion loss of $Ni_{(1-x)}Cu_xMn_2O_4$ $(0 \leq x \leq 1)$ fritless thick films were calculated from transmission coefficient of the sample using the formula,

$$\text{Insertionloss} = -20 \log \frac{V_T}{V_I}$$

where, V_T is transmitted output power by thick film, V_I is the incident power on thick film.

Figure 6 shows the insertion loss as well as absorption loss of $Ni_{(1-x)}Cu_xMn_2O_4$ $(0 \leq x \leq 1)$ thick films in the frequency range 8.2 GHz to 18 GHz. From the figure it is seen that in the frequency range 8.2 GHz to 11 GHz composition dependent variations in both insertion loss and absorption loss are observed.

The composition with $x = 0.4$ shows the largest absorption. At 12 GHz the insertion loss is minimum ~ 5 dB indicating that the $Ni_{(1-x)}Cu_xMn_2O_4$ thick film is least absorbing (absorption loss maxima). Between 11.5 to 16 GHz the absorption becomes high again, but it is not composition dependent. At ~ 17 GHz again composition dependent effects are obtained, with the absorption being larger for the composition $x = 0.4$. The high absorption (low absorption loss) in a large band of frequencies indicates potential for microwave applications [17]. Absorption is the heat loss under the action between electric dipole or magnetic dipole in material and the electromagnetic field. Such materials can be a good thermistor material in the

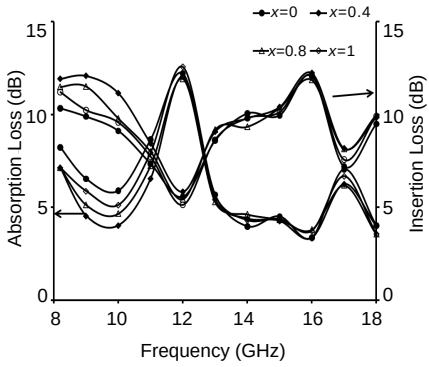

Figure 6. Microwave absorption loss and insertion loss of fritless $Ni_{(1-x)}Cu_xMn_2O_4$ thick film.

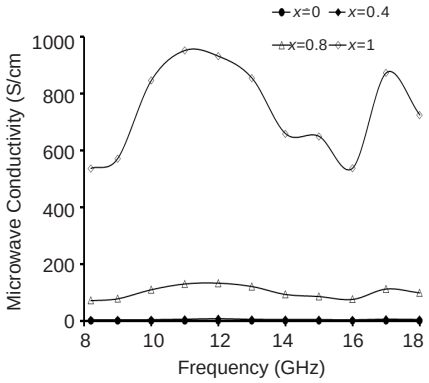

Figure 7. Microwave conductivity of fritless $Ni_{(1-x)}Cu_xMn_2O_4$ thick film.

microwave range.

The microwave conductivity of fritless $Ni_{(1-x)}Cu_xMn_2O_4$ ($0 \leq x \leq 1$) thick film was calculated using the equation according to Ramey et al. [18] using the transmittance data.

$$\frac{\sigma}{\sigma_0} = 1 + \frac{3}{4}\left(k - \frac{k^3}{12}\right)E_i - \left(\frac{3}{8k}\right)\left(1 - e^{-k}\right) - \left[\frac{5}{8} + \left(\frac{k}{16}\right) - \left(\frac{k^2}{16}\right)\right]e^{-k}$$

where 'σ_0' is bulk conductivity, 'k' $= d/l_0$ where 'd' is the film thickness and 'l_0' is the mean free path. And 'E_i' is the transmittance.

From Fig. 7, it is observed that as copper content increases microwave conductivity also increases. The conductivity varies from ~ 1 S/cm for the composition $x = 0$, ~ 8 S/cm for $x = 0.4$, > 70 S/cm for $x = 0.8$ and > 500 S/cm for $x = 1.0$. As copper content increases the frequency dependent variations are increased. Conduction is caused by the hopping of electrons between the Mn^{3+} and Mn^{4+} on octahedral sites. In other words it is Mn^{3+}+Cu^{2+}+$Mn^{4+} \leftrightarrow Mn^{4+}$+ Cu^{+}+ Mn^{4+} and Mn^{3+}+Cu^{2+}+$Mn^{4+} \leftrightarrow Mn^{4+}$+ Cu^{2+}+ Mn^{3+}. Both Mn and Cu cations at the octahedral sites acts as hopping ions to cause an increase in the conductivity. To the authors knowledge there are no reports available on the microwave conductivity of fritless $Ni_{(1-x)}Cu_xMn_2O_4$ thick film in the 8–18 GHz frequency range.

The microwave conductivity of alumina substrate was calculated by two ways (i) real part of conductivity ($\sigma = \omega\varepsilon_0\varepsilon''$) and (ii) conductivity calculated by Ramey's formula. In Ramey's paper the formula illustrated for the calculation of conductivity is for thin

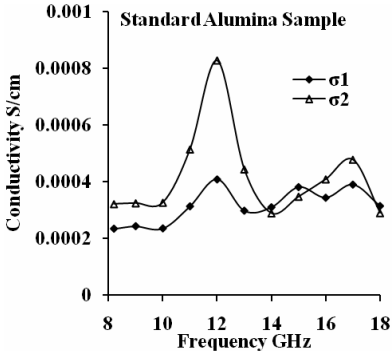

Figure 8. Microwave conductivity of alumina substrate, where $\sigma 1$ is real part of conductivity ($\sigma = \omega\varepsilon_0\varepsilon''$) and $\sigma 2$ is the conductivity calculated by Ramey's formula.

conductor films. But in this paper we applied this formula for a standard dielectric alumina sample for 8–18 GHz frequency range. Comparing both Ramey's and using dielectric formula, the values obtained by both are well in agreement with each other which is shown in Fig. 8. Hence, we applied this standardized method to our dielectric nickel manganite thick films.

The dielectric constant of fritless $Ni_{(1-x)}Cu_xMn_2O_4$ thick film was measured using VSWR measurement setup. The VSWR measurement setup was almost the same as the waveguide reflectometer setup, instead of two 3 dB directional couplers VSWR slotted section was used. Initially the slotted section was calibrated with air and alumina. The alumina and manganite thick films acts as a load to the transmission of the microwaves and microwaves reflected back from that load. The positions of the minima of the standing wave were compared with that of air. As impedance is mismatched, the position of the minima is shifted by placing the thick films as load. The reflection coefficient was also measured. The Smith chart was used to find the phase change due to the fritless $Ni_{(1-x)}Cu_xMn_2O_4$ ($0 \leq x \leq 1$) thick film in the path of microwaves and permittivity measured by using the formula [19].

$$\varepsilon' = \left(1 + \frac{\Delta\phi\lambda_0}{360d}\right)^2 \quad \text{and} \quad \varepsilon'' = \frac{\Delta\phi\lambda_0\sqrt{\varepsilon'}}{8.686\pi d}$$

where '$\Delta\phi$' is phase difference between incident and reflected waves; 'λ_0' is guided wavelength. And 'd' is thickness of the sample.

The calculated ε' and ε'' are plotted in Figs. 9(a) and (b); it is

observed that as Cu concentration increases dielectric constant also increases. The value of ε' lies in the range 6 to 19.5, and ε'' is in between 0.0391 to 0.1875.

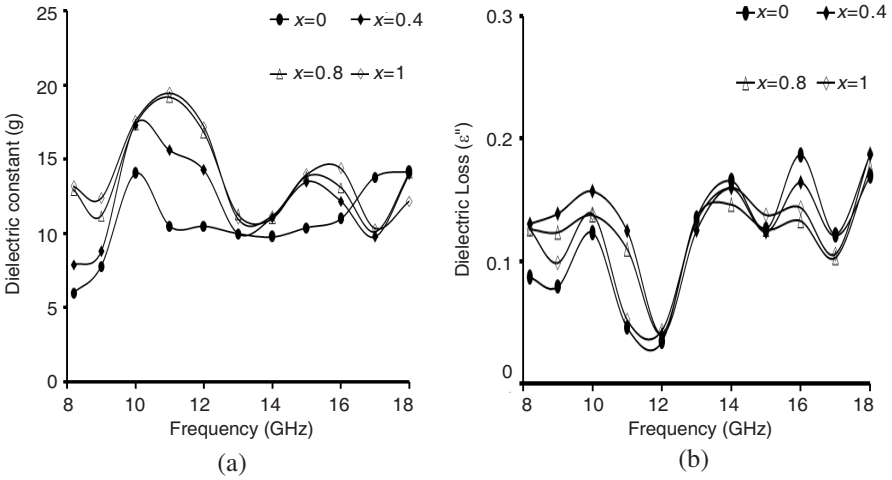

Figure 9. (a) Microwave dielectric constant of the fritless $Ni_{(1-x)}Cu_xMn_2O_4$ thick film. (b) Microwave dielectric loss of the fritless $Ni_{(1-x)}Cu_xMn_2O_4$ thick film.

The microwave permittivity of $Ni_{(1-x)}Cu_xMn_2O_4$ ($0 \leq x \leq 1$) thick film depends on the shape and size of the grains. It is well known that as polarization increases dielectric constant also increases, and polarization is affected by structural homogeneity, stoichiometry, density, grain size and porosity [16]. Due to increase in copper content the structural homogeneity decreases which may cause a slight increase in polarization.

In fritless $Ni_{(1-x)}Cu_xMn_2O_4$ thick film due to Cu content the grain size increases (SEM Fig. 2) and anisotropy decreases which is responsible for the increase in dielectric constant. According to Zaki [20] the substitution of Cu ions cause the formation of vacancies, if the formed vacancies are cations then ε' increases. The decrease in the intensity of peak 645 cm^{-1} (Fig. 4) with copper content is due to Mn-O bond strength in this region being weaker, which results in larger polarization and hence higher dielectric constant for higher copper concentration.

From Fig. 9(a), the dielectric constant shows peaking behavior at lower frequency. It is observed that for lower copper concentration ($x \leq 0.4$) dielectric constant peak is observed at 10 GHz but when copper content increases ($x \geq 0.8$) it shifts towards higher frequency

up to 11 GHz. The shift of the dielectric peak to higher frequency with increasing copper concentration is attributed to the corresponding increase in the mobility of the charge carriers.

In case of the dielectric loss (ε'') (Fig. 9(b)) as frequency increases in the 8–12 GHz range loss decreases and becomes minimum at 12 GHz. Beyond this the loss again increases. Below 12 GHz the thick film with composition $x = 0.4$ shows larger loss, whereas above 12 GHz the film with $x = 0.0$ shows slightly larger loss as compared to other compositions. The absorption data (Fig. 6) also show similar frequency dependent effects.

4. CONCLUSION

The fritless $Ni_{(1-x)}Cu_xMn_2O_4$ ($0 \leq x \leq 1$) thick film synthesized by oxalic precursor method shows absorbing nature over a large range of frequency in the X and Ku band region of the electromagnetic spectrum. It has spinel structure and porous morphology, the grain size increasing with copper content. The microwave permittivity of $Ni_{(1-x)}Cu_xMn_2O_4$ ($0 \leq x \leq 1$) thick films increases with increase in copper concentration. The microwave conductivity also increases with the increase in copper content. The fritless $Ni_{(1-x)}Cu_xMn_2O_4$ ($0 \leq x \leq 1$) thick film with $x = 0.4$ shows the best absorption properties useful for application as planar thermistor material for microwave power measurement.

ACKNOWLEDGMENT

One of the authors, Dr. Vijaya Puri, gratefully acknowledges UGC for the award of research scientist 'B' and financial assistance under UGC-DRS-SAP II.

REFERENCES

1. Chamaani, S., S. A. Mirtaheri, M. Teshnehlab, M. A. Shoorehdeli, and V. Seydi, "Modified multi-objective particle swarm optimization for electromagnetic absorber design," *Progress In Electromagnetics Research*, PIER 79, 353–366, 2008.
2. Abbas, S. M., A. K. Dixit, R. Chatterjee, and T. C. Goel, "Complex permittivity and microwave absorption properties of $BaTiO_3$-polyaniline composite," *Materials Science and Engineering B*, Vol. 125, 167–171, 2005.

3. Zhang, Y. C., Z. X. Yue, X. Qi, B. Li, Z. L. Gui, and L. T. Li, "Microwave dielectric properties of $Zn(Nb_{1-x}Ta_x)_2O_6$ ceramics," *Materials Letters*, Vol. 58, 1392–1395, 2004.
4. Chou, Y.-H., M.-J. Jeng, Y.-H. Lee, and Y.-G. Jan, "Measurement of RF PCB dielectric properties and losses," *Progress In Electromagnetics Research Letters,* Vol. 4, 139–148, 2008.
5. He, X., Z. X. Tang, B. Zhang, and Y. Q. Wu, "A new deembedding method in permittivity measurement of ferroelectric thin film material," *Progress In Electromagnetics Research Letters,* Vol. 3, 1–8, 2008.
6. Marie, M., J. Mazzochette, A. H. Feingold, P. Amstutz, R. L. Wahlers, C. Huang, and S. J. Stein, "Thick film variable temperature variable attenuators," *Proceeding of the 1997 IMPS Philadelphia Symposium*, Vol. 3235, 344–349, 1997.
7. Savic, S. M., M. V. Nikolic, O. S. Aleksic, M. Slankamenac, M. Zivanov, and P. M. Nikolic, "Intrinsic resistivity of sintered nickel manganite vs. powder activation time and density," *Science of Sintering*, Vol. 40, 27–32, 2008.
8. Verses, A., J. G. Noudem, O. Pery, S. Founez, and G. Bailleul, "Manganese based spinel — Like ceramics with NTC — Type thermistor behavior," *Solid State Ionics*, Vol. 178, 423–428, 2007.
9. Park, K., "Structural and electrical properties of $FeMg_{0.7}Cr_{0.7-x}Al_xO_4$ ($0 \leq y \leq 0.3$) thick film NTC thermistors," *Journal of European Ceramic Society*, Vol. 256, 909–914, 2006.
10. Kanade, S. A. and V. Puri, "Properties of thick film $Ni_{0.6}Co_{0.4}Fe_yMn_{2-y}O_4$: ($0 \leq y \leq 0.5$) NTC ceramics," *Journal of Alloys and Compounds*, Vol. 475, 352–355, 2009.
11. Pi, L., X. Xu, and Y. Zhang, "Anomalous transport properties of heavily doped polycrystalline $La_{0.825}Sr_{0.175}Mn_{1-x}Cu_xO_3$," *Physical Review B*, Vol. 62, 5667–5672, 2000.
12. Julien, C., M. Massot, S. Rangan, M. Lemal, and D. Guyomard, "Study of structural defects in -MnO_2 by Raman spectroscopy," *Journal of Raman Spectroscopy*, Vol. 33, 223–228, 2002.
13. Chitra, S., P. Kalyani, T. Mohan, M. Massot, S. Ziolkiewicz, R. Ganandharan, M. Eddrief, and C. Julien, "Physical properties of $LiMn_2O_4$ spinel prepared at moderate temperature," *Ionics*, Vol. 4, 8–15, 1998.
14. Dokko, K., M. Mohamed, N. Anzue, T. Itoh, and I. Uchida, "In situ Raman apectroscopic studies of $LiNi_xMn_{2-x}O_4$ thin film cathod materials for lithium ion secondary batteries," *Journal of*

Materials Chemistry, Vol. 12, 3688–3693, 2002.

15. Li, W. J., B. Zang, and W. Lu, "Structural properties and Raman spectroscopy of $La_{(2+4x)/3}Mn_{1-x}Cu_xO_3$ $(0 \leq x \leq 0.2)$," *Physics Letters A*, Vol. 362, 327–330, 2007.
16. Dimri, M., A. Verma, S. Kashyap, D. Dube, O. Thakur, and C. Prakash, "Structural, dielctric and magnetic properties of NiCuZn ferrite grown by citrate precursour mehod," *Materials Science and Engineering B*, Vol. 133, 42–48, 2006.
17. Li, G., G. G. Hu, H. D. Zhou, X. J. Fan, and X. G. Li, "Absorption of microwaves in $La_{1-x}Sr_xMnO_3$ manganese powders over a wide bandwidth," *Journal of Applied Physics*, Vol. 90, 5512–5514, 2001.
18. Ramey, R. and T. Lewis, "Properties of thin metal films at microwave frequencies," *Journal of Applied Physics*, Vol. 39, 1747–1752, 1968.
19. Kim, J. H., K. B. Kim, and S. H. Noh, "New density independent model for measurement of grain moisture content using microwave techniques," *Journal of Electronics Engineering and Information Science*, Vol. 2, 72–78, 1997.
20. Zaki, H. M., "AC conductivity and frequency dependence of the dielctric properties for copper doped magnetite," *Physica B*, Vol. 363, 232–244, 2005.